JACS
JOURNAL OF THE AMERICAN CHEMICAL SOCIETY

COMMUNICATION

pubs.acs.org/JACS

Nanoparticle-Driven Assembly of Block Copolymers: A Simple Route to Ordered Hybrid Materials

Ying Lin,[†] Vikram K. Daga,[‡] Eric R. Anderson,[†] Samuel P. Gido,[†] and James J. Watkins*[,†]

[†]Department of Polymer Science and Engineering and [‡]Department of Chemical Engineering, University of Massachusetts Amherst, 120 Governors Drive, Amherst, Massachusetts 01003, United States

Supporting Information

ABSTRACT: The addition of nanoparticles that selectively hydrogen bond with one of the segments of a block copolymer is shown to induce order in otherwise disordered systems. This enables the fabrication of well-ordered hybrid materials with spherical, cylindrical, or lamellar domains at particle loadings of more than 40%, as evidenced by TEM and SAXS. The approach described is simple and applicable to a wide range of nanoparticles and block copolymers, and it lays the groundwork for the design of cooperatively assembled functional devices.

The preparation of well-ordered hybrid polymer/inorganic nanostructures with exceptional control over size, shape, composition, and organization of nanoscale domains is central to the development of next-generation materials and devices for energy generation and storage, microelectronics, communications, photonics, and other applications.[1] While the desired structures can often be identified, their realization via practical fabrication methods has remained challenging, especially for those cases that require high concentrations of nanoparticles (NPs) within ordered periodic structures.

The incorporation and distribution of NPs and other nanoscale additives within block polymers (BCPs) has evolved into an area of considerable research,[2] and comprehensive reviews are available.[3] In principle, microphase-segregated BCP melts are ideal templates for these applications because of their ability to form periodic spherical, cylindrical, bicontinuous, and lamellar morphologies spontaneously at precisely controllable domain sizes.[4] However their utility for this purpose is ultimately subject to success in controlling the partitioning and loading of the additives within the target domains. The distribution of NPs, the degree of order realizable within the composite, and the maximum loading of NPs are determined largely by a balance of enthalpic contributions resulting from interactions of the polymer chain segments with the NP surface or ligands bound to the NP surface and entropic contributions. The entropic considerations include not only those of mixing and translational entropy of the particles but also, and importantly, the penalties associated with perturbations in chain conformation due to chain stretching to accommodate the NPs.[3a,b,5] For systems in which the interactions between NPs and chain segments are enthalpically neutral or weak, the entropic penalties associated with chain stretching impose an upper bound on the NP loading.

The location of NPs within BCP hosts at relatively low NP loadings can be influenced by the use of NP ligands that are compatible with one or more of the blocks.[2d,e,h,6] NPs containing ligand systems that are compatible with both blocks in an A−B type copolymer, for example, can be selective for the interface. These interfacially active particles can mediate interactions between the copolymer segments and control the domain orientation[7] and morphology. The use of ligands that are compatible with only one of the blocks can lead to preferential segregation of the NPs within the compatible domain. In a system where the ligand is chemically identical to one of the blocks, the particle−polymer interaction is enthalpically neutral,[2d] and both theory and experiment indicate that the NP distribution within the domain depends on the particle size.[2e,5a,8] Nonetheless, the addition of each enthalpically neutral particle carries an entropic penalty that pushes the system closer to disorder, ultimately limiting the loading to a few volume % on a NP core (ligand-free) basis.

To achieve high NP loadings while maintaining strong segregation in the composite, one must either alleviate the BCP chain stretching penalty or offset it. Recently, Zhao et al.[9] reported the assembly of ordered polymer/NP assemblies in which the particles reside within domains consisting of short organic side chains associated with one of the BCP segments in the hierarchical assembly via hydrogen bonding. While the interaction between the particles and side chains is weak, the prevalence of chain ends may reduce the stretching penalty. Surprisingly, very little work has been directed toward employing strong favorable interactions between NPs and the host BCP to offset the entropic penalty associated with their addition. In one report, Warren et al.[10] prepared mesoporous metals in which metal NPs coated with an organic shell consisting of ionic liquid coatings were coassembled with specially designed poly(isoprene-*b*-dimethylaminoethyl methacrylate) BCPs. While their system employed specific chemistries and somewhat cumbersome processing, it did yield ordered assemblies.

Here we present a general approach for the preparation of well-ordered polymer/NP composites through the concept of additive-driven assembly. We recently demonstrated that small-molecule additives or homopolymers with multiple H-bond-donating groups such as carboxylic acids and phenol can induce microphase segregation of otherwise disordered Pluronic BCP poly(ethylene oxide-*b*-propylene oxide-*b*-ethylene oxide) (PEO-*b*-PPO-*b*-PEO) surfactant melts.[11] Hydrogen-bond-mediated interactions between ordered BCP systems and small-molecule additives have previously been shown by others to produce novel supramolecular architectures.[12−14] For example, Ikalla and ten Brinke[12] and Meijer and co-workers[13] have shown that the addition of small molecules that form hydrogen bonds with one of the blocks can alter the phase behavior to induce order-to-order transitions and achieve

Received: January 13, 2011
Published: April 11, 2011

dx.doi.org/10.1021/ja2003632 | *J. Am. Chem. Soc.* 2011, 133, 6513–6516

Scheme 1. Schematic Representation of NP-Driven Assembly of BCPs via H-Bonding

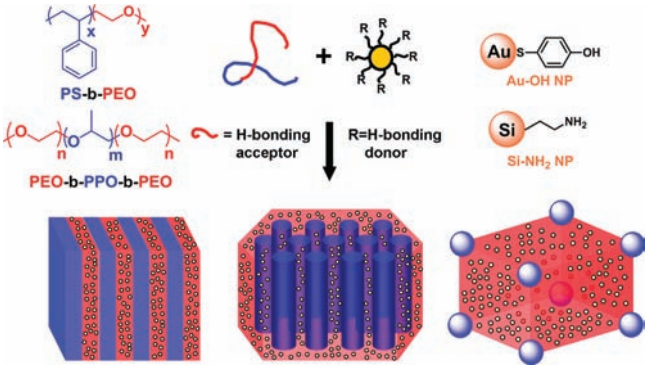

new hierarchical structures or to achieve lattice structures that are difficult or impossible to obtain in the neat diblock copolymer. Our additive-driven approach differs from these strategies in that NPs bearing multiple H-bonding interactions are chosen primarily to induce order in otherwise disordered materials (or strengthen phase segregation in ordered materials) while either maintaining morphologies encountered in neat BCPs or potentially accessing new ones.

We use multipoint, enthalpically favorable interactions between NPs functionalized with short H-bond-donating ligands and a H-bond-accepting BCP segment. This approach strengthens phase segregation and enables NP loadings of 40 wt % in blends (Scheme 1). We illustrate this approach using Au and Si NPs containing ligands bearing phenol or amine groups that drive the assembly of otherwise disordered PEO-*b*-PPO-*b*-PEO triblock and poly(styrene-*b*-ethylene oxide) (PS-*b*-PEO) diblock copolymers. This approach not only enables the preparation of well-ordered composites at high NP loadings but also demonstrates increases in segregation strength upon NP addition, and we believe it is the first example of additive-induced ordering by NP addition.

4-Hydroxythiophenol-functionalized Au (Au−OH) NPs[15] and allylamine-functionalized Si (Si−NH_2) NPs formed via hydrosilylation to yield covalent ligand attachment[16] were prepared using literature procedures. Thermogravimetric analysis (TGA) indicated that the Au content of the Au−OH NPs was ∼72.3 wt % and that the Si core represented ∼60.1 wt % of the Si−NH_2 NPs. The BCP templates were a PS-*b*-PEO BCP [M_n = 8.6 kDa, PDI = 1.05, PEO weight fraction (f_{PEO}) = 0.56; denoted as PS3.8k-*b*-PEO4.8k] and the PEO-*b*-PPO-*b*-PEO triblock copolymers Pluronic F127 (M_n = 12.0 kDa, PDI = 1.26, f_{PEO} = 0.70) and F108 (M_n = 14.6 kDa, PDI = 1.23, f_{PEO} = 0.80) obtained from BASF. We tailored the size of the NPs to be compatible with the domain sizes of the BCPs chosen for the study. For example, the radius of gyration (R_g) of the PEO block of F108 (11.6 kDa) is on the order of ∼5 nm [$R_g = \alpha(N/6)^{1/2}$]. Consequently, we prepared NPs with diameters of 2−3 nm. See the Supporting Information (SI) for detailed characterization of the NPs.

Figure 1a shows small-angle X-ray scattering (SAXS) profiles for PS3.8k-*b*-PEO4.8k and blends of this BCP with Au−OH NPs at several NP concentrations. In this paper, we express the concentrations of the NPs primarily as the weight % of the composite based on the mass of the NP core and ligand shell. The TGA data and BCP composition then yield the NP core loading on a ligand-free basis in the composite and in the target domain. The latter is a good measure of the efficacy of NP incorporation (see Tables S2−S5 in the SI). The volume % of the NPs (core + ligand shell) can be estimated using the TGA data and the densities of the components and is the most relevant parameter for assessing the influence of NP loading on the morphology of the composite. This value is provided in parentheses following the first mention of the NP weight % for each composite.[17]

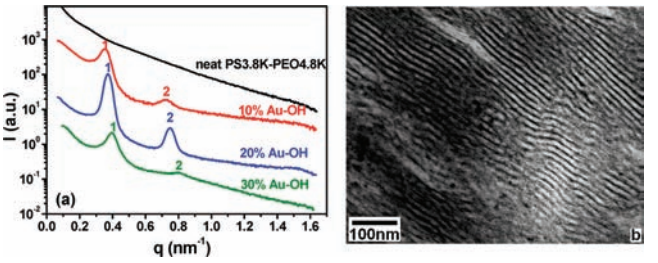

Figure 1. (a) SAXS profiles of PS3.8k-*b*-PEO4.8k with Au−OH NPs at 0, 10, 20, and 30 wt % concentration. (b) TEM image of a blend of F108 with 30 wt % Au−OH NPs.

Neat PS3.8k-*b*-PEO4.8k was disordered in the melt because of its low molecular weight and thus low segregation strength. The addition of 10 wt % (3.0 vol %) Au−OH NPs induced an ordering transition, indicating that the addition of the NPs causes microphase segregation in the otherwise disordered melt. Moreover, the scattering data showed a second-order peak at a q value double that of the first, suggesting a lamellar morphology. Transmission electron microscopy (TEM) (Figure 1b) confirmed this structural characterization. This lamellar morphology was maintained when the NP concentration was increased to 30 wt % (10.5 vol %). When normalized for the mass fraction of PEO in the template, the concentration of Au−OH NPs in the target domain approached 43.4 wt % (31.4 wt % or 2.5 vol % on a ligand-free basis).

It is informative to contrast the behavior of the Au−OH/PS3.8k-*b*-PEO4.8k composites with that of systems in which the NP−BCP interactions are weak or enthalpically neutral. Thiyagarajan[18] reported that the addition of polystyrene (PS)-functionalized Au NPs to a strongly segregated PS-*b*-poly(2-vinylpyridine) copolymer progressively weakened the phase segregation as the volume fraction of NPs increased, eventually resulting in disorder. The opposite trend is evident in Figure 1, which demonstrates that the addition of Au−OH NPs to PS3.8k-*b*-PEO4.8k induced an ordering transition and strengthened the domain segregation at loadings up to >20%. TEM analysis of the Au−OH/PS3.8k-*b*-PEO4.8k system was performed to gain insight into the distribution of NPs. Bright-field TEM images of the unstained samples prepared by microtoming (Figure 1b and Figure S4 in the SI) revealed a lamellar morphology, consistent with the SAXS data. The high contrast in the absence of staining is a clear indication that Au NPs were not dispersed throughout the whole BCP but were selectively segregated in one domain.

Since PS3.8k-*b*-PEO4.8k is not commercially available, we looked to a more readily available system that would be scalable and amenable to large-volume applications, including roll-to-roll processing. Pluronic BCPs are inexpensive and available in large quantities with various compositions and molecular weights. Because of their relatively low molecular weights and the chemical similarity of the blocks, Pluronic BCPs exhibit weak segregation; the goal here was to induce stronger segregation and order with the addition of H-bonding NPs. Figure 2a shows SAXS profiles for blends of F108 and Au−OH NPs at several compositions. Neat F108 exhibited a broad peak due to the correlation hole effect observed for disordered BCPs.[4c,19] Upon addition of 10 wt % (3.0 vol %) Au−OH NPs, the primary peak sharpened, indicating an increase in the segregation

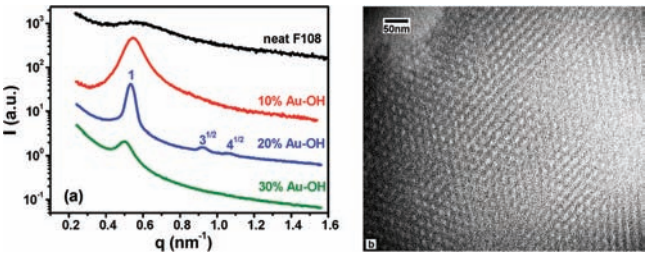

Figure 2. (a) SAXS profiles of F108 blended with Au−OH NPs at 0, 10, 20, and 30 wt % concentration. (b) TEM image of a blend of F108 with 20 wt % Au−OH NPs (100000× magnification).

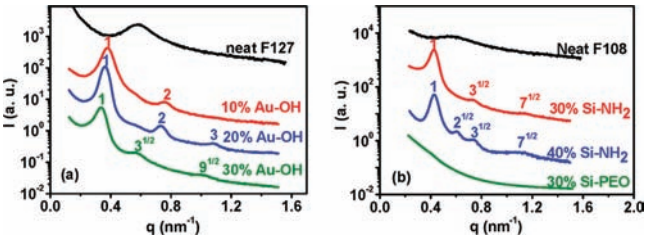

Figure 3. (a) SAXS profiles of F127 with Au−OH NPs at 0, 10, 20, and 30 wt % concentration. (b) SAXS profiles of F108 with Si−NH_2 NPs at 0, 30, and 40 wt % concentration and with PEO-terminated Si NPs at 30 wt % concentration.

strength. At 20 wt % (6.4 vol %) Au−OH NPs, multiple scattering peaks were observed at q = 0.535, 0.929, and 1.07 nm^{-1} (peak position ratios relative to q^* of 1, $3^{1/2}$, $7^{1/2}$, ... with a d spacing of 11.8 nm ($d_{100} = 2\pi/q^*$). These higher-order reflections resulted from structural correlations with hexagonal symmetry, suggesting a cylindrical structure with significantly stronger domain segregation than at lower NP loadings. Further addition of NPs up to 30 wt % (10.5 vol %) led to a loss of the multiple higher-order reflections, suggesting an upper bound on the particle loading at which strong order can be maintained in this system.

Figure 2b shows a TEM image of a microtomed sample of F108 blended with 20 wt % Au−OH NPs. Since F108 is PEO-rich, the NP-loaded PEO phase forms the matrix and PPO is the minor (cylindrical) domain. The TEM image, in combination with the SAXS data, indicates hexagonally packed PPO cylinders embedded in a PEO−NP matrix. We note that since PEO and PPO have similar electron densities, the contrast observed in the TEM image is due to Au NPs residing exclusively in the PEO domains. (Figure S5 shows a TEM image acquired over a larger area.) Well-ordered NP/BCP composites with domain sizes below 10 nm have not been previously achieved, in part because of reductions in the segregation strength of the BCP template resulting from reductions in the molecular weight of the template required to achieve small d spacings. In the current method, the effective copolymer segregation strength is increased by the NP additive. This offers a desirable avenue for exploration of NP arrays with small features.

This strategy was also generally applicable to other Pluronic BCP surfactants. For example, Au−OH NPs were blended with F127, a Pluronic containing 70 wt % PEO, and the resulting SAXS profiles of the blends with Au−OH NPs as a function of composition are shown in Figure 3a. Addition of 10 wt % Au−OH NPs resulted in the formation of a microphase-separated lamellar system. At 20 wt %, a well-ordered lamellar morphology with three orders of reflection and a d spacing of 18.2 nm was formed. Interestingly, upon an increase in the concentration of Au NPs to 30 wt %, a transition from lamellar to cylindrical morphology with a d spacing of 19.0 nm occurred. This additive-induced ordering transition was driven by both an increase in the effective interaction parameter and changes in the overall volume fraction between the two microphase-segregated domains.

The preparation of well-ordered composites requires component mobility during assembly, which can be achieved by thermal annealing or annealing in the presence of solvent. Figure S6 shows SAXS data for F127 with 20 wt % phenol-terminated Au NPs acquired after annealing of the composites at 70 °C for periods of up to 48 h. The strength of segregation and order in the composite improved with annealing time up to 36 h. Extended exposure of thiol-functionalized Au NPs to elevated temperatures, however, can lead to deboning of ligands by thermally activated cleavage of Au−thiol bonds, as has been noted in some references.[20] This may ultimately limit annealing times and conditions for systems containing these NPs.

To demonstrate the generality of using favorable H-bonding interactions to facilitate NP loading and segregation of NP/BCP blends, we investigated the incorporation of Si NPs bearing short-chain amines. With the microemulsion method of Tilley,[16] 2−3 nm amine-terminated silicon nanocrystals were synthesized. Ligand attachment via the formation of Si−C bonds was achieved via hydrosilylation with allylamine, as described in the SI. Figure 3b compares SAXS profiles of neat Pluronic F108 surfactant and its blends with Si NPs decorated with allylamine ligands, which serve as H-bond donors. The addition of Si−NH_2 NPs induced microphase segregation in F108, resulting in the formation of well-ordered morphologies, as indicated by the sharpening of the first peak and appearance of multiple higher-order reflections. At 30 wt % (26.2 vol %) Si−NH_2 NPs, the peak position ratios (1, $3^{1/2}$, $7^{1/2}$, ...) indicated the formation of a cylindrical morphology. Since the Si−NH_2 NPs were expected to be selectively partitioned into the PEO phase, the volume fraction of the PEO phase increased with Si−NH_2 NP loading, and therefore the morphology changed from cylindrical to spherical at 40 wt % (35.5 vol %), as indicated by the peak position ratios (1, $2^{1/2}$, $3^{1/2}$, $7^{1/2}$, ...). When normalized for the mass fraction of PEO in the template, the concentration of Si NPs (core + ligand) in the target domain approached 45.5 wt % (equivalent to 27.3 wt % or 13.4 vol % within the PEO domains on a ligand-free basis). As a control experiment, PEO-functionalized Si NPs were blended with F108 at 30 wt % (26.1 vol %) concentration. A broadening of the primary peak was observed iin the SAXS results. This illustrates the importance of the favorable interaction through H-bonding.

The strength of the interactions of the additives with the PEO chain segments and their interaction with the PEO phase was investigated using differential scanning calorimetry (DSC).[21] The DSC thermograms obtained between −80 and 80 °C for neat F108 and its blends with 30 and 40 wt % Si−NH_2 NPs are shown in Figure S12. Neat F108 is characterized by a melting endotherm at 56.5 °C associated with melting of PEO crystallites. PPO does not crystallize and therefore shows no melting. Neat F108 is disordered, and therefore, a single T_g was observed at −70.2 °C. At both 30 and 40 wt % loading of Si−NH_2 NPs in F108, no crystallite melting transition was observed for PEO, while a T_g was visible at about −20 °C. Suppression of

dx.doi.org/10.1021/ja2003632 |J. Am. Chem. Soc. 2011, 133, 6513–6516

crystallization of PEO implies that the additives have molecular-scale interactions with the PEO chains.

In summary, we have presented a pathway for achieving well-ordered hybrid materials. NPs functionalized with groups that exhibit strong H-bonds to the hydrophilic block of BCPs can enhance the segregation strength and induce microphase segregation and order in otherwise disordered BCPs. We have illustrated this approach using Au and Si NPs containing ligands bearing phenol and amine groups to drive the assembly of otherwise disordered PEO-*b*-PPO-*b*-PEO triblock and PS-*b*-PEO diblock copolymers. The approach enables Au NP loadings of up to 30 wt % (10.5 vol %) and Si NP loadings of up to 40 wt % (35.5 vol %) in the composites, as evidenced by the SAXS and TEM data. Beyond providing advantages enabling the assembly of nanostructured devices, the strategy and material sets are readily scalable and amenable to roll-to-roll processing.

■ ASSOCIATED CONTENT

Supporting Information. Experimental information; TEM, IR, and TGA characterization of NPs; additional SAXS data; and TEM images of the blends. This material is available free of charge via the Internet at http://pubs.acs.org.

■ AUTHOR INFORMATION

Corresponding Author
watkins@polysci.umass.edu

■ ACKNOWLEDGMENT

This work was supported by the NSF Center for Hierarchical Manufacturing at the University of Massachusetts (CMMI-0531171).

■ REFERENCES

(1) (a) Huynh, W. U.; Dittmer, J. J.; Alivisatos, A. P. *Science* **2002**, *295*, 2425. (b) Lopes, W. A.; Jaeger, H. M. *Nature* **2001**, *414*, 735. (c) Park, S.; Lee, D. H.; Xu, J.; Kim, B.; Hong, S. W.; Jeong, U.; Xu, T.; Russell, T. P. *Science* **2009**, *323*, 1030. (d) De Rosa, C.; Auriemma, F.; Di Girolamo, R.; Pepe, G. P.; Napolitano, T.; Scaldaferri, R. *Adv. Mater.* **2010**, *22*, 5414. (e) Xiang, J.; Lu, W.; Hu, Y.; Wu, Y.; Yan, H.; Lieber, C. M. *Nature* **2006**, *441*, 489. (f) Briseno, A. L.; Yang, P. *Nat. Mater.* **2009**, *8*, 7. (g) Rancatore, B. J.; Mauldin, C. E.; Tung, S.-H.; Wang, C.; Hexemer, A.; Strzalka, J.; Fréchet, J. M. J.; Xu, T. *ACS Nano* **2010**, *4*, 2721.

(2) (a) Gaines, M. K.; Smith, S. D.; Samseth, J.; Bockstaller, M. R.; Thompson, R. B.; Rasmussen, K. O.; Spontak, R. J. *Soft Matter* **2008**, *4*, 1609. (b) Kang, H.; Detcheverry, F. A.; Mangham, A. N.; Stoykovich, M. P.; Daoulas, K. C.; Hamers, R. J.; Müller, M.; de Pablo, J. J.; Nealey, P. F. *Phys. Rev. Lett.* **2008**, *100*, No. 148303. (c) Lee, J. Y.; Shou, Z.; Balazs, A. C. *Phys. Rev. Lett.* **2003**, *91*, No. 136103. (d) Chiu, J. J.; Kim, B. J.; Kramer, E. J.; Pine, D. J. *J. Am. Chem. Soc.* **2005**, *127*, 5036. (e) Chiu, J. J.; Kim, B. J.; Yi, G. R.; Bang, J.; Kramer, E. J.; Pine, D. J. *Macromolecules* **2007**, *40*, 3361. (f) Costanzo, P. J.; Beyer, F. L. *Macromolecules* **2007**, *40*, 3996. (g) Matsen, M. W.; Thompson, R. B. *Macromolecules* **2008**, *41*, 1853. (h) Zou, S.; Hong, R.; Emrick, T.; Walker, G. C. *Langmuir* **2007**, *23*, 1612. (i) Kim, B. J.; Bang, J.; Hawker, C. J.; Kramer, E. J. *Macromolecules* **2006**, *39*, 4108.

(3) (a) Bockstaller, M. R.; Mickiewicz, R. A.; Thomas, E. L. *Adv. Mater.* **2005**, *17*, 1331. (b) Balazs, A. C.; Emrick, T.; Russell, T. P. *Science* **2006**, *314*, 1107. (c) Haryono, A.; Binder, W. H. *Small* **2006**, *2*, 600. (d) Shenhar, R.; Norsten, T. B.; Rotello, V. M. *Adv. Mater.* **2005**, *17*, 657. (e) Mezzenga, R.; Ruokolainen, J. *Nat. Mater.* **2009**, *8*, 926. (f) Sudeep, P. K.; Emrick, T. *ACS Nano* **2009**, *3*, 2870.

(4) (a) Bates, F. S.; Fredrickson, G. H. *Phys. Today* **1999**, *52*, 32. (b) Binder, K. *Adv. Polym. Sci.* **1994**, *112*, 181. (c) Leibler, L. *Macromolecules* **1980**, *13*, 1602.

(5) (a) Huh, J.; Ginzburg, V. V.; Balazs, A. C. *Macromolecules* **2000**, *33*, 8085. (b) Lee, J.-Y.; Thompson, R. B.; Jasnow, D.; Balazs, A. C. *Phys. Rev. Lett.* **2002**, *89*, No. 155503.

(6) (a) Kim, B. J.; Chiu, J. J.; Yi, G. R.; Pine, D. J.; Kramer, E. J. *Adv. Mater.* **2005**, *17*, 2618. (b) Li, Q. F.; He, J. B.; Glogowski, E.; Li, X. F.; Wang, J.; Emrick, T.; Russell, T. P. *Adv. Mater.* **2008**, *20*, 1462. (c) Tsutsumi, K.; Funaki, Y.; Hirokawa, Y.; Hashimoto, T. *Langmuir* **1999**, *15*, 5200. (d) Zhang, Q. L.; Gupta, S.; Emrick, T.; Russell, T. P. *J. Am. Chem. Soc.* **2006**, *128*, 3898.

(7) Lin, Y.; Boker, A.; He, J. B.; Sill, K.; Xiang, H. Q.; Abetz, C.; Li, X. F.; Wang, J.; Emrick, T.; Long, S.; Wang, Q.; Balazs, A.; Russell, T. P. *Nature* **2005**, *434*, 55.

(8) (a) Bockstaller, M. R.; Lapetnikov, Y.; Margel, S.; Thomas, E. L. *J. Am. Chem. Soc.* **2003**, *125*, 5276. (b) Mackay, M. E.; Tuteja, A.; Duxbury, P. M.; Hawker, C. J.; Van Horn, B.; Guan, Z.; Chen, G.; Krishnan, R. S. *Science* **2006**, *311*, 1740.

(9) Zhao, Y.; Thorkelsson, K.; Mastroianni, A. J.; Schilling, T.; Luther, J. M.; Rancatore, B. J.; Matsunaga, K.; Jinnai, H.; Wu, Y.; Poulsen, D.; Fréchet, J. M. J.; Alivisatos, A. P.; Xu, T. *Nat. Mater.* **2009**, *8*, 979.

(10) Warren, S. C.; Messina, L. C.; Slaughter, L. S.; Kamperman, M.; Zhou, Q.; Gruner, S. M.; DiSalvo, F. J.; Wiesner, U. *Science* **2008**, *320*, 1748.

(11) (a) Daga, V. K.; Watkins, J. J. *Macromolecules* **2010**, *43*, 9990. (b) Tirumala, V. R.; Daga, V.; Bosse, A. W.; Romang, A.; Ilavsky, J.; Lin, E. K.; Watkins, J. J. *Macromolecules* **2008**, *41*, 7978. (c) Tirumala, V. R.; Romang, A.; Agarwal, S.; Lin, E. K.; Watkins, J. J. *Adv. Mater.* **2008**, *20*, 1603.

(12) (a) Ruokolainen, J.; Mäkinen, R.; Torkkeli, M.; Mäkelä, T.; Serimaa, R.; ten Brinke, G.; Ikkala, O. *Science* **1998**, *280*, 557. (b) van Zoelen, W.; Asumaa, T.; Ruokolainen, J.; Ikkala, O.; ten Brinke, G. *Macromolecules* **2008**, *41*, 3199. (c) Bondzic, S.; de Wit, J.; Polushkin, E.; Schouten, A. J.; ten Brinke, G.; Ruokolainen, J.; Ikkala, O.; Dolbnya, I.; Bras, W. *Macromolecules* **2004**, *37*, 9517.

(13) Sijbesma, R. P.; Beijer, F. H.; Brunsveld, L.; Folmer, B. J. B.; Hirschberg, J. H. K. K.; Lange, R. F. M.; Lowe, J. K. L.; Meijer, E. W. *Science* **1997**, *278*, 1601.

(14) Tang, C.; Lennon, E. M.; Fredrickson, G. H.; Kramer, E. J.; Hawker, C. J. *Science* **2008**, *322*, 429.

(15) Brust, M.; Fink, J.; Bethell, D.; Schiffrin, D. J.; Kiely, C. *J. Chem. Soc., Chem. Commun.* **1995**, 1655.

(16) Warner, J. H.; Hoshino, A.; Yamamoto, K.; Tilley, R. D. *Angew. Chem., Int. Ed.* **2005**, *44*, 4550.

(17) The relative volumes of the particle core and ligand can vary widely among NP systems and can be controlled over broad ranges within a single class of NPs (e.g., Au−PS in Table 1 of ref 2i). Thus, the equivalent volume % of the NPs (core + shell) can yield very different NP core loadings on a ligand-free basis, even within a single class of NPs.

(18) Lo, C. T.; Lee, B.; Pol, V. G.; Rago, N. L. D.; Seifert, S.; Winans, R. E.; Thiyagarajan, P. *Macromolecules* **2007**, *40*, 8302.

(19) Zhang, F.; Stühn, B. *Colloid Polym. Sci.* **2006**, *284*, 823.

(20) (a) Listak, J.; Hakem, I. F.; Ryu, H. J.; Rangou, S.; Politakos, N.; Misichronis, K.; Avgeropoulos, A.; Bockstaller, M. R. *Macromolecules* **2009**, *42*, 5766. (b) Teranishi, T.; Hasegawa, S.; Shimizu, T.; Miyake, M. *Adv. Mater.* **2001**, *13*, 1699.

(21) Tirumala, V. R.; Pai, R. A.; Agarwal, S.; Testa, J. J.; Bhatnagar, G.; Romang, A. H.; Chandler, C.; Gorman, B. P.; Jones, R. L.; Lin, E. K.; Watkins, J. J. *Chem. Mater.* **2007**, *19*, 5868.